JGR Biogeosciences

RESEARCH ARTICLE
10.1029/2024JG008168

Climatic Drivers for the Variation of Gross Primary Productivity Across Terrestrial Ecosystems in the United States

Yan Chen[1], **Guiling Wang**[2], **and Anji Seth**[1]

[1]Department of Geography, University of Connecticut, Storrs, CT, USA, [2]Department of Civil and Environmental Engineering, University of Connecticut, Storrs, CT, USA

Key Points:

- Light use efficiency (LUE) variation is generally driven by temperature in spring and by water stress in summer
- Soil water availability dominates the LUE response to moderate droughts, but vapor pressure deficit becomes important under extreme drought
- The primary drivers of LUE variation also depend on background climate and vegetation types

Supporting Information:

Supporting Information may be found in the online version of this article.

Correspondence to:

Y. Chen and G. Wang,
yanc1002@uconn.edu;
guiling.wang@uconn.edu

Citation:

Chen, Y., Wang, G., & Seth, A. (2024). Climatic drivers for the variation of gross primary productivity across terrestrial ecosystems in the United States. *Journal of Geophysical Research: Biogeosciences*, *129*, e2024JG008168. https://doi.org/10.1029/2024JG008168

Received 29 MAR 2024
Accepted 22 JUL 2024

Author Contributions:

Conceptualization: Guiling Wang
Data curation: Yan Chen
Formal analysis: Yan Chen
Methodology: Yan Chen, Guiling Wang, Anji Seth
Project administration: Guiling Wang
Resources: Guiling Wang
Software: Yan Chen
Supervision: Guiling Wang, Anji Seth
Validation: Yan Chen, Guiling Wang
Visualization: Yan Chen
Writing – original draft: Yan Chen, Guiling Wang, Anji Seth
Writing – review & editing: Yan Chen, Guiling Wang, Anji Seth

Abstract Temperature and water stress are important factors limiting the gross primary productivity (GPP) in terrestrial ecosystems, yet the extent of their influence across ecosystems remains uncertain. This study examines how surface air temperature, soil water availability (SWA) and vapor pressure deficit (VPD) influence ecosystem light use efficiency (LUE), a critical metric for assessing GPP, across different ecosystems and climatic zones at 80 flux tower sites based on in situ measurements and data assimilation products. Results indicate that LUE increases with temperature in spring, with higher correlation coefficients in colder regions (0.79–0.82) than in warmer regions (0.68–0.78). LUE reaches a plateau earlier in the season in warmer regions. LUE variations in summer are mainly driven by SWA, exhibiting a positive correlation indicative of a water-limited regime. The relationship between the daily LUE and daytime temperature shows a clear seasonal hysteresis at many sites, with a higher LUE in spring than in fall under the same temperature, likely resulting from younger leaves being more efficient in photosynthesis. Drought stress influences LUE through SWA in all ranges of water availability; VPD variation under moderate conditions does not have a clear influence on LUE, but extremely high VPD (exceeding the threshold of 1.6 kPa, often observed during extreme drought-heat events) causes a dramatic reduction of LUE. Our findings provide insight into how ecosystem productivities respond to climate variability and how they may change under the influence of more frequent and severe heat and drought events projected for the future.

Plain Language Summary The terrestrial ecosystem assimilates carbon through photosynthesis, and its ability to convert sunlight energy to primary production during photosynthesis is commonly measured by light use efficiency (LUE). To understand how temperature, water in the soil, and atmospheric aridity impact carbon assimilation through photosynthesis, we analyzed the drivers of LUE at 80 sites across different ecosystems and different climate regimes in the United States. We found that temperature is the main factor influencing LUE of grassland and forest in spring, and has a greater influence on LUE in colder regions than in warmer regions. Under the same temperature, LUE in the spring is higher than in the autumn season, likely because of new leaves. In summer, deep soil water availability is the primary driver of LUE variations. In addition, extreme aridity of the atmosphere contributes to a dramatic decrease in LUE during compound heat-drought events. Our findings contribute to advancing our understanding of how climatic factors influence LUE across different ecosystems in a changing climate.

1. Introduction

In the United States, the terrestrial ecosystem carbon sink amounts to 360 Tg C per year, offsetting ~25% of fossil fuel emissions and playing an essential role in climate change mitigation (Hayes et al., 2018). However, there is a large range of uncertainty in land carbon uptake estimation and projection (Bodman et al., 2013). Furthermore, the increasing occurrence of extreme events such as drought, heat, and extreme rainfall due to global warming has disturbed the seasonal and interannual carbon dynamics, resulting in significant uncertainties in terrestrial carbon uptake estimation (Turner et al., 2021; Wolf et al., 2016).

The effect of temperature on photosynthesis through physiological processes has been widely documented (Hu et al., 2021; Kirschbaum, 2004). Temperature affects photosynthesis through two primary mechanisms: direct biochemical effects and indirect stomatal effects (Lloyd & Farquhar, 2008). The direct effect is related to the biochemical process of photosynthesis at the leaf level, which is usually described by two key kinetic variables, the maximum rate of Rubisco carboxylation (Vcmax) and the maximum rate of electron transport (Jmax), both of

which are sensitive to temperature (Bernacchi et al., 2001, 2003; Moore et al., 2021). With the rise of temperature, the Vcmax and the Jmax increase, reaching their maximum level at the optimal temperature, which causes the photosynthetic rate to peak (Pau et al., 2018). In addition, both optimal temperature and photosynthesis capacity acclimate to growth temperatures (Crous et al., 2022). Additionally, an increase in air temperature with unchanged relative humidity leads to an increase in the vapor pressure deficit (VPD), and excessive VPD may induce stomatal closure thus reducing stomatal conductance, leading to a decrease in plant photosynthesis. This indirect mechanism further exacerbates the negative effects of higher-than-optimal temperature on plant photosynthesis (Dusenge et al., 2021). Some studies suggested that the stomatal conductance response to increased temperature and moisture limitation, rather than the thermal acclimation of photosynthesis, dominates the photosynthesis performance at the ecosystem level (Kullberg et al., 2023; Way & Yamori, 2014).

However, the effects of temperature on gross primary productivity (GPP) can vary significantly across different ecosystems and environmental conditions. In certain ecosystems, especially those in colder regions, a rise in temperature can result in a notable increase in GPP, as warmer temperatures enhance photosynthesis and prolong the growing season. Conversely, in ecosystems located in hot regions, the opposite effect may occur (Choury et al., 2022; Pau et al., 2018; Zhang et al., 2017). The optimal temperature in photosynthesis varies across locations and ecosystems, generally lower in cool regions or high elevation and higher in warmer regions (Chen et al., 2021; Niu et al., 2012). In some tropical regions, the optimal temperature is close to the growing season air temperature (Huang et al., 2019).

Drought influences GPP through both increased VPD and reduced soil moisture. VPD increases during drought, resulting from both low levels of atmospheric/soil moisture and the often concurrent high temperature. High VPD can accelerate transpiration and further exacerbates water stress in the soil (Grossiord et al., 2020; Sun & Wang, 2022); excessive VPD also reduces stomatal opening or conductance thus slowing down photosynthesis. Soil water deficit during drought can also limit photosynthesis and reduce plant carbon uptake through physiological mechanisms. However, previous studies reached no consensus on the separate and joint effects of temperature, VPD, and soil water stress on GPP across temporal and spatial scales. Some studies show stronger effects of VPD on interannual variability of GPP than other environmental variables (He et al., 2022; Sulman et al., 2016), while others highlight the dominant role of soil moisture in determining long-term variability in GPP (Green et al., 2019; Humphrey et al., 2021; Liu et al., 2020). The challenge lies in distinguishing the degree to which GPP is affected by soil moisture and atmospheric aridity, because of the intricate interactions between the two and how they vary across plant species, soil types, and climatic conditions (Wang et al., 2022).

Furthermore, surface soil moisture and air temperature exhibit a strong correlation in ecosystems that are water-limited, and their impact on GPP varies across different biomes and timescales. From previous studies, the response of GPP to warming and water availability varies along climate gradients. Ecosystems in colder and wetter regions demonstrate higher sensitivity to changes of temperature, while those in warmer and drier regions are more sensitive to soil moisture changes (Higgins et al., 2023; Peñuelas et al., 2007, 2009). For ecosystems where both temperature and water availability are important drivers of light-use efficiency (LUE) variation, the LUE relationship with either one of the variables is confounded by the other as the two are tightly coupled at the process level. High temperature may accelerate the depletion of soil moisture through evaporation; low soil moisture can increase temperature by limiting the evaporative cooling.

The plant physiological responses to environmental stressors are highly variable, depending on species and background climate, among others (Fang et al., 2014; Von Buttlar et al., 2018). For example, plant species have evolved in different ecological niches and adapted to varying environmental conditions (Gratani, 2014; Stubbs et al., 2018; Turcotte et al., 2012). Some plant species have developed mechanisms to tolerate water stress, such as deep root systems, drought-resistant leaves, and the ability to close stomata to conserve water (Seleiman et al., 2021). Under persistent changes of environmental conditions, vegetation grown at different temperatures responds differently to temperature changes. For instance, plants living in cool environments, when adapting to elevated temperatures, exhibit a rise in optimum temperature, with no concurrent alteration in their photosynthetic capacity (Yamasaki et al., 2002). The response of GPP to water and heat stress also varies between vegetation types. Grasses respond rapidly to heat and dryness, with a correspondingly rapid decrease in GPP; in contrast, trees exhibit delayed responses to these stresses, which can be attributed to their more complex physiological responses, including modifications to leaf structure and function, alterations in the expression of stress-responsive genes, and changes in the activity of enzymes involved in photosynthesis and respiration (Hu et al., 2022). Trees

and grass differ in enzyme distribution and the response of rubisco activity to changes in temperature, light, nitrogen deposition, and CO_2 concentration (Lu et al., 2022). Furthermore, trees may adjust the allocation of resources between different organs, such as roots and leaves, to optimize their ability to acquire and utilize water and nutrients in response to environmental stresses (Rennenberg et al., 2006; Wolf et al., 2013). Thus, although the response of photosynthetic capacity to short-term temperature anomalies is clear, the mechanisms underlying the plant photosynthesis response to environmental factors at the inter-annual and longer time scales are complex and difficult to discern based on observations.

This study aims to identify the dominant climatic drivers of the interannual variation of photosynthesis across terrestrial ecosystems in the United States, and to assess how multiple factors may interact to shape the terrestrial ecosystem response to compound heat-drought events.

2. Data and Methodology

We selected a total of 84 observation sites that had at least four years of data during 2001–2020 from the Ameriflux database (see Table S1). The selected sites included evergreen needle-leaf forests (ENF), deciduous broadleaf forests (DBF), mixed forests (MF), and grasslands (GRA). However, only 43 out of the 84 flux tower sites have GPP_NT_VUT_REF data (GPP, which is derived from the nighttime respiration partitioning approach) published in the Ameriflux database. Therefore, we utilized the GPP data from FLUXCOM, a gridded global carbon and energy product derived by upscaling flux tower data using machine learning, and chose the grid cells where the 84 flux towers are located. These data are presumably more reliable than those in grid cells that contain no flux tower site. While cross-validation at the data production stage revealed that FLUXCOM effectively captures the GPP inter-site variability and seasonal patterns (Jung et al., 2019), here we conduct further validation and quality control. Of the 43 flux tower sites with GPP_NT_VUT_REF data, only those with measured (QC = 0) or good-quality gap-filled (QC = 1) data are chosen, which exclude four sites lacking good-quality data during the study period. Additionally, we also excluded three MF sites and four sites (US-xML, US-xSB, US-Var, US-ONA) with a lower-than-0.8 correlation coefficient (r) between GPP from FLUXCOM and GPP_NT_VUT_REF (see Table S1). For the remaining 32 sites, we calculated the LUE using the GPP_NT_VUT_REF and FLUXCOM GPP data respectively, and compared their relationships with temperature in spring and soil water availability in summer (Figures S2 and S3 in Supporting Information S1). The results reveal a striking similarity between the two sources of data. FLUXCOM GPP data proves to be fit for purpose in this study. For soil moisture, data is unavailable for many sites; among the sites where data is available, the soil measurement depth varies considerably from site to site. We therefore took the soil moisture data from NLDAS Phase 2 (NLDAS2), which were simulated by the Mosaic land-surface model (NLDAS project, 2022; Xia et al., 2012). To assess the potential uncertainties related to soil moisture data, we conducted a comparative analysis using measurements from 13 flux tower sites (chosen based on data availability) that have consistent soil profiles and soil moisture measurements up to the depth of 2 m. We then examined how the relationship between light use efficiency (LUE) and soil water content (SWC) differed when using SWC data from NLDAS2 relative to field data at the 13 flux tower sites (see Figure S1 in Supporting Information S1). Despite the fact that NLDAS2 tends to underestimate SWC, the relationship between LUE and SWC, as well as the SWC variations, are similar when using the two sources of soil moisture data. It is therefore reasonable to utilize NLDAS2 data when investigating the role of SWC in LUE variation at the interannual timescale. Additionally, we use half-hourly temperature and VPD data from the Ameriflux data set to derive their daytime (between 7:00 a.m. and 17:00 p.m.), monthly, and seasonal values (see Table 1).

To better understand the impact of temperature and drought on the plant carbon uptake in various regions of the United States and to exclude the impact of potential adaptation to background climate, we divided the study domain into three sub-regions based on gradients of temperature and water availability (Figure 1). Specifically, we divided the domain into northern and southern regions considering the vast temperature contrast; we then further subdivided the southern region, as the southwest is drier than the southeast. Environmental factors influencing GPP were highly region-dependent and vegetation-dependent. For example, vegetation in arid regions can adapt to water shortage through physiological strategies, while vegetation in moist regions does not show a rapid response to reduction in soil moisture, as the soil water availability is high to start with, providing some buffering zone (Sun et al., 2021; Vicente-Serrano et al., 2013). Furthermore, the GPP of grassland responds to drought more rapidly than forests (Sun et al., 2021), and GPP response to temperature in different regions can even show opposite signs (Zhou et al., 2017). Dividing the study domain into subregions allowed us to focus on the specific mechanisms underlying

Journal of Geophysical Research: Biogeosciences

10.1029/2024JG008168

Table 1
Data Used in This Study

Data set	Type	Variables	Resolution	Frequency	Record length	References
FLUXCOM	Tower data upscaled to grid	GPP	0.0833° × 0.0833°	Daily and Monthly	2000/01–2020/12	Jung (2020)
Ameriflux	In situ measurement	GPP	–	Half hourly	Site specific	ameriflux.lbl.gov
Ameriflux	In situ measurement	VPD	–	Half hourly	Site specific	ameriflux.lbl.gov
Ameriflux	In situ measurement	Temperature	–	Half hourly	Site specific	ameriflux.lbl.gov
Ameriflux	In situ measurement	Soil moisture	–	Half hourly	Site specific	ameriflux.lbl.gov
CERES	Satellite	PAR direct/diffuse fluxes	1° × 1°	Daily and Monthly	2001/03–2020/12	Doelling et al. (2016)
North American Land Data Assimilation System (NLDAS-2)	Model simulation	Soil moisture (SM) (0–10 cm), (0–200 cm)	0.125° × 0.125°	Monthly	2001/01–2020/12	(NLDAS project (2022); Xia et al. (2012)
NLDAS Mosaic Soil Hydraulic Properties Dataset	Observations	Wilting point (WP)	0.125° × 0.125°	Static	–	Mitchell et al. (2004)
NLDAS Mosaic Soil Hydraulic Properties Dataset	Observations	Porosity (0–10 cm), (10–40 cm), (40–200 cm)	0.125° × 0.125°	Static	–	Mitchell et al. (2004)
AVHRR	Satellite	Leaf Area Index (LAI)	0.05°	Daily	2001/01–2020/12	Vermote and NOAA CDR Program (2019)

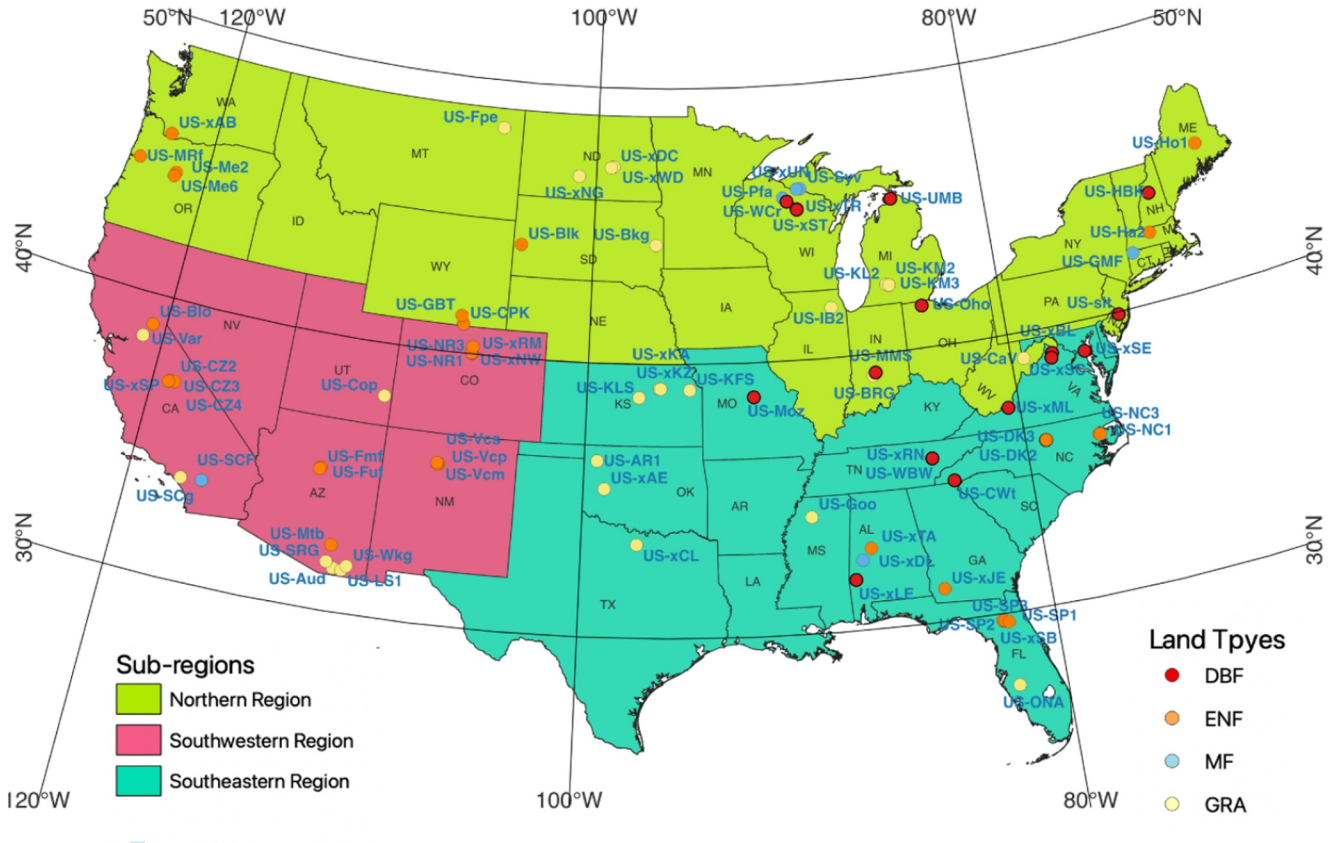

Figure 1. Flux tower distribution and ecosystem types employed in this study.

the response of plant carbon uptake to temperature, soil water stress and atmospheric aridity with minimal confounding effects from the contrasting climate regimes.

We use the LUE as an ecosystem performance metric. Conceptually, LUE reflects the ability of plants to convert light energy into biomass (Monteith, 1972); in practice, multiple definitions exist in the literature (Gitelson & Gamon, 2015), some based on incident PAR, some based on absorbed PAR (APAR), which is calculated as the product of PAR and fraction of absorbed PAR, while others based on PAR absorbed by green vegetation only. Which definition to use is often dictated by the purpose of a study. Assuming a constant vegetation structure (i.e., neglecting the inter-annual variation of leaf area index in each season), a decrease of APAR caused by heat or water stress may cause a proportional decrease of GPP, leading to a relatively stable GPP/APAR. To capture physiological responses to environmental stress, in this study we define LUE as GPP/PAR. This lumps the direct physiological response with the indirect impact of canopy structure response that results from the temporal accumulation of physiological effects. For example, severe reduction of GPP would slow down canopy growth and reduce leaf area index (LAI); this, when not accounted for, may lead to a slight overestimation of the physiological sensitivity. Where appropriate, we also analyze LUE divided by LAI to eliminate the impact of canopy structure changes.

$$\mathrm{LUE} = \frac{\mathrm{GPP}}{\mathrm{PAR\ Direct\ Flux} + \mathrm{PAR\ Diffuse\ Flux}} \tag{1}$$

The total PAR, which is the sum of the direct and diffuse components of PAR from CERES SYN1Deg-Month, is used to compute the monthly and seasonal mean values of LUE for each site throughout the time period of data availability.

The soil water availability for plants depends on soil moisture and soil hydraulic properties (Mohammadi Alagoz et al., 2022; Pinno & Wilson, 2013). Accounting for the impact of porosity and wilting point (WP), we estimate

the soil water availability (SWA) for the top 10 cm ($SWA_{shallow}$) and top 200 cm (SWA_{deep}) separately using Equations 2 and 3:

$$SWA_{shallow} = \frac{SM_{10cm} - WP}{Porosity_{10cm} - WP} \quad (2)$$

$$SWA_{deep} = \frac{SM_{200cm} - WP}{Porosity_{200cm} - WP} \quad (3)$$

Here SM_{10cm} and SM_{200cm} represent soil moisture in the top 10 cm and top 200 cm of the soil, respectively, $Porosity_{10cm}$ and $Porosity_{200cm}$ denote the corresponding porosity, and WP is the wilting point. In NLDAS2, the soil moisture and porosity vary with depth while wilting point remains the same across all soil layers. The layer thickness-weighted average of soil moisture and porosity through the top 10 and 200 cm are used to calculate the $SWA_{shallow}$ and SWA_{deep}, respectively. SWA ranges between 0 and 1, with values close to 1 indicating no water stress and values close to 0 indicating severe water stress for plants.

To account for potential dependency on vegetation type, we categorized the sites according to land cover, including ENF, DBF, MF, and GRA. This categorization allowed us to compare ecohydrological responses across these diverse ecosystems. To account for potential seasonal dependency, we divided the data into spring (MAM), summer (JJA), and autumn (SON). To identify the climatic drivers of LUE, we first examined the relationship between LUE and daytime temperature at the daily timescale. The Pearson regression model was then utilized to assess the LUE correlations with temperature and $SWA_{deep}/SWA_{shallow}$ for different seasons and vegetation types separately. Furthermore, to comprehensively examine the roles played by temperature and SWA, we binned the monthly LUE data according to the combination of temperature (with a bin size of 4°C) and SWA (with a bin size of 0.1); for seasons and ecosystems where temperature is not a strong control, we binned LUE according to the combination of VPD (with a bin size of 0.4 kPa) and either temperature (with a bin size of 4°C) or SWA (with a bin size of 0.1) to analyze the role of VPD in the vegetation response to drought.

3. Results

3.1. LUE-Temperature Relationship at Daily Timescale

At the process level, LUE increases with temperature up to a certain value and decreases when temperature exceeds an optimum that varies with vegetation type and background climate. Using six sites (US-Vcm, US-Vcp, US-xSP, US-Cop, US-Me2, and US-Me6) as examples, Figure 2a shows at the daily timescale how LUE varies with daytime mean temperature. The optimal daytime mean temperature for photosynthesis varies among sites, ranging from 15°C to 25°C. Note that not all sites experienced a decrease in LUE at high temperatures. The sites where temperature can reach the optimum are mainly ENF and GRA ecosystems in the arid and semi-arid regions of the western United States. Other than temperature, another factor that may contribute to a decrease of LUE is light saturation. Radiation is a confounding factor for the LUE-temperature relation since radiation is in the denominator for LUE while high radiation and high temperature may coincide. To assess the potential role of light saturation, we analyzed the variability of GPP across different combinations of temperature and PAR in spring and summer for six sites experiencing a decrease of daily LUE with temperature (Figure S4 in Supporting Information S1). In spring for all sites, the results indicate no heat stress and no PAR saturation. In summer, GPP decreases on high-temperature days regardless of PAR values at all six sites, and continues to increase with PAR through the full range of PAR variation at four of the six sites. At the remaining two sites (US-Vcm and US-Vcp) in summer, while the largest GPP decrease is associated with high temperature, GPP indeed shows some degree of light saturation when PAR exceeds 150 W/m^2. This indicates that the compound effect of light saturation and heat stress drives the decrease in LUE during summer at US-Vcm and US-Vcp, while for the other four sites, the decrease in LUE is driven by high temperatures alone. Notably, the apparent threshold of PAR value (150 W/m^2) is close to the summertime daily-average clear-sky PAR of ~160 W/m^2 over the continental U.S. (Frouin & Pinker, 1995).

At any given temperature, there is an enormous range of day-to-day LUE variability that reflects the impact of weather-related noises in factors other than temperature. To extract a systematic signal of influence, we examined

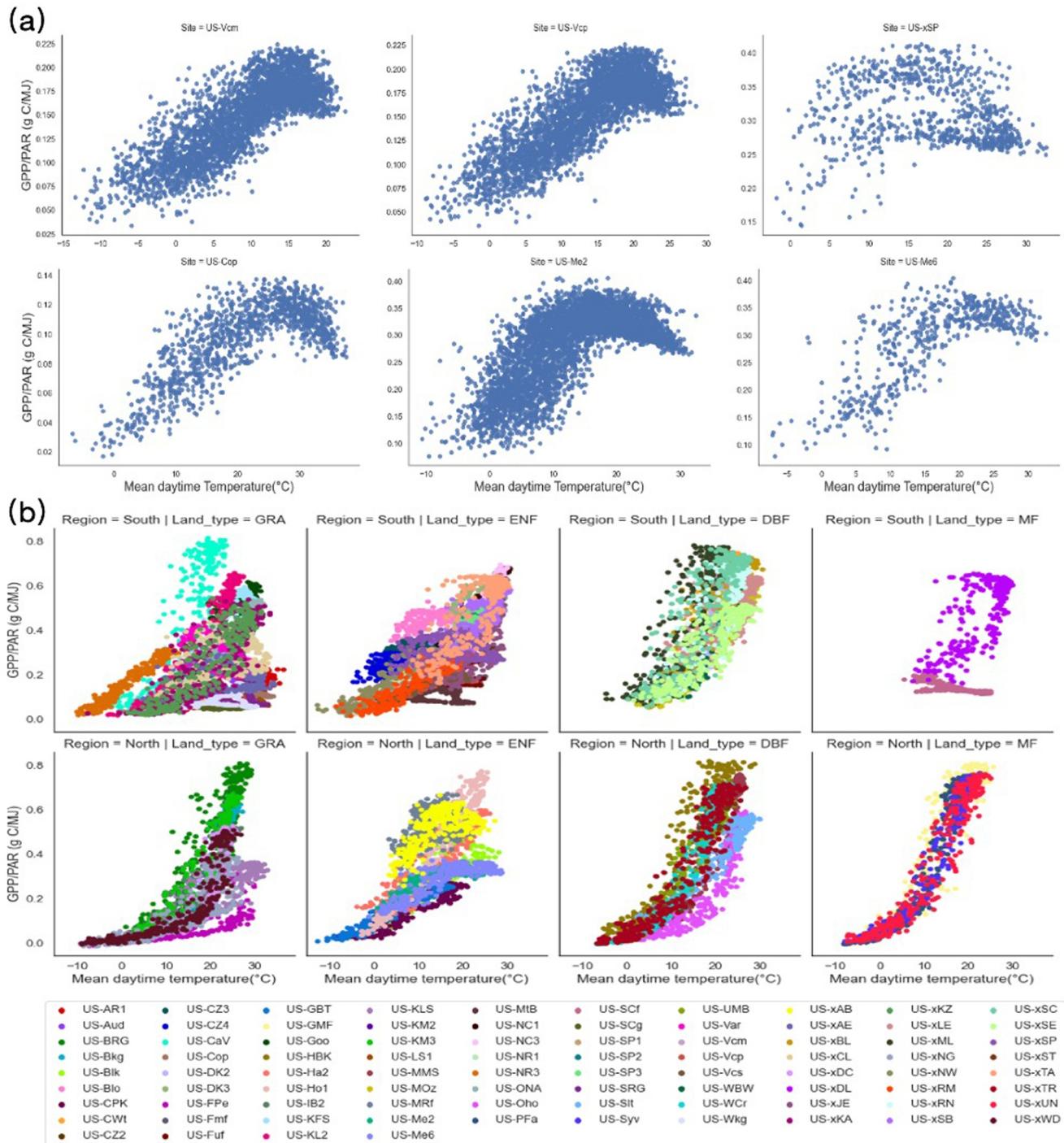

Figure 2. (a) The relationship between LUE and daytime temperature during March to November at six sites, including US-Vcm, US-Vcp, US-xSP, US-Cop, US-Me2, and US-Me6, where each data point represents a daily value; (b) the relationship between the daily climatological LUE and daytime temperature during March to November, where different flux tower sites are distinguished by color.

the temperature dependency of LUE based on the 20-year mean climatology of the daily LUE data and compared different sites of the same ecosystem type within the same region (Figure 2b). Taking the multi-year averaging for each Julian day led to a well-defined relationship linking LUE with temperature at each site, with a relatively small spread at each given temperature. However, the multi-year averaging also eliminated the segment of the

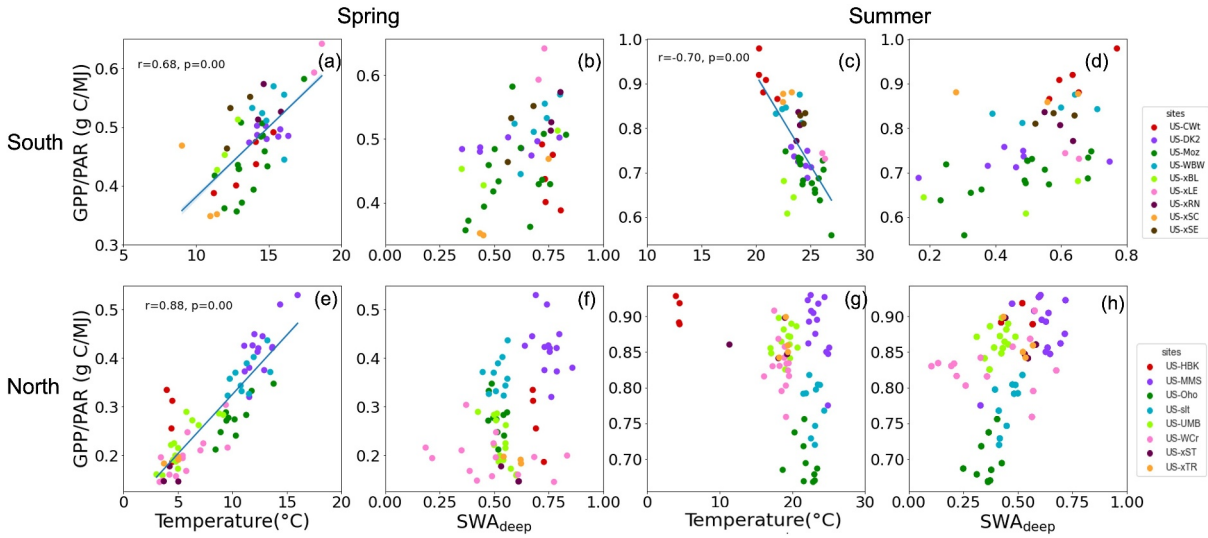

Figure 3. The relationship between seasonal mean LUE and seasonal mean temperature and SWA_{deep} in DBFs during spring and summer in the Southern US (a)–(d) and Northern US (e)–(h), where different flux tower sites are distinguished by color. The values in panels are for the Pearson correlation coefficient (r) and its significance level (p).

relationship that featured a negative impact of high temperature on LUE, which suggests that the decrease at high temperature shown in Figure 2a only occurred during days or months of extreme temperature anomalies (which may become more frequent in a warmer climate) and does not reflect the climatological norm. Instead, at most sites under normal conditions, LUE increases with temperature in the spring, plateaus as temperature reaches the optimal in summer, and decreases in the fall season as temperature cools. Generally, LUE reaches the plateau at temperatures between 25°C and 30°C across all ecosystems, but at an earlier time at southern sites (spring) than at northern sites (summer) (Figure S5 in Supporting Information S1).

Interestingly, at most sites, the LUE - temperature relationship shows a hysteresis loop. Under the same temperature, LUE in the fall season is lower than in the spring, and the magnitude of the hysteresis loop is site-dependent. The hysteresis behavior could result from seasonal differences in radiation, leaf area index, and soil water content. However, defining LUE as GPP divided by PAR removes most of the solar radiation effects already, which eliminates solar radiation difference as a possible cause; when normalizing LUE by LAI, the spring-fall contrast remains or gets even more evident, which eliminates LAI difference as a possible cause (Figure S6 in Supporting Information S1). The hysteresis behavior in the LUE-temperature relationship is likely because younger leaves are less prone to photoinhibition than older leaves (Bielczynski et al., 2017), making the spring leaves more effective at carbon uptake. Another potential cause for this seasonal disparity is the impact of other environmental factors such as water stress difference between spring and fall (Liu et al., 2023; Niu et al., 2011). Given the seasonal dependence of LUE sensitivity, we will use monthly data for the remainder of our analysis and separate the analysis by season to assess the impact of climate-related variability and extremes.

3.2. Climatic Drivers of LUE Variability

We employed the LUE-Temperature and LUE-SWA analyses to identify the environmental factors that drive the variation in LUE across different ecosystems during spring and summer respectively. SWA_{deep} is used for forest sites; for grassland sites, $SWA_{shallow}$ is used in wet regions, and SWA_{deep} is used in dry regions.

DBF sites are prevalent in the eastern United States, characterized by a humid climate and strong temperature seasonality. Figure 3 shows a clear temperature-driven LUE response during spring and summer, without strong limitation by SWA. In spring during the transition from the cold winter to warm summer, LUE increased from nearly 0 to ∼0.6 g C/MJ as temperature rose from 3°C to 17°C in the northern region and from 8°C to 20°C in the south. The correlation of LUE with temperature is stronger in the north (with a correlation coefficient of 0.88) than in the south (r = 0.68), as temperature sets a stronger constraint for growth in the colder climate.

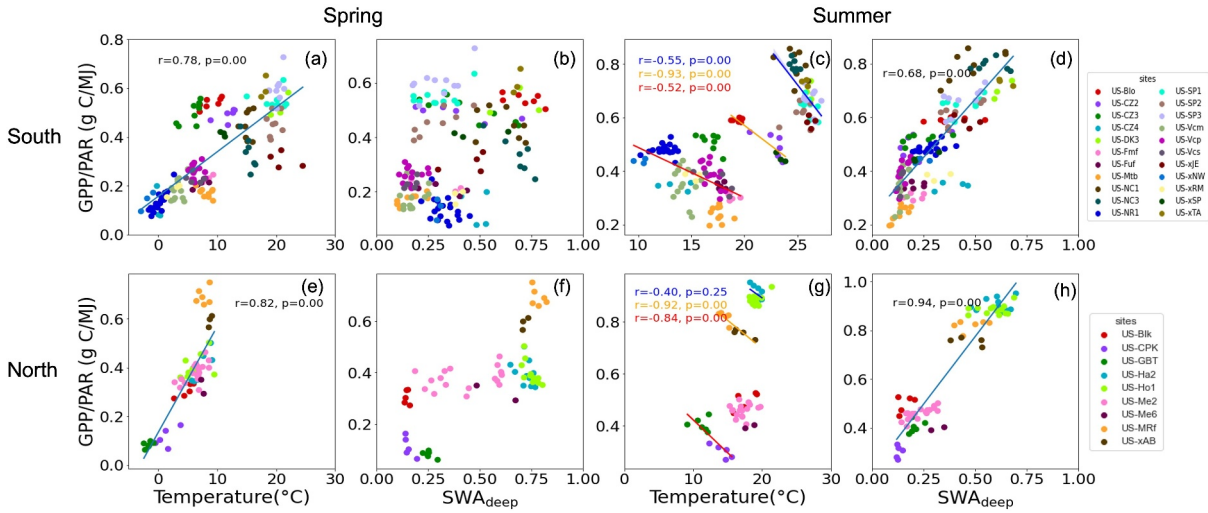

Figure 4. The relationship between seasonal mean LUE and seasonal mean temperature and SWA$_{deep}$ in ENFs during spring and summer in the Southern US (a)–(d) and Northern US (e)–(h), where different flux tower sites are distinguished by color. The values in panels are for the Pearson correlation coefficient (r) and its significance level (p).

During summer, southern DBFs experience heat stress when seasonal mean temperatures exceed 20°C, which leads to a decrease in LUE. However, DBFs in the north, with temperatures between 15°C and 27°C, do not show a consistent, unambiguous response to temperature and SWA. Instead, LUE is rather high, ranging from 0.65 to 0.95 g C/MJ, which can be explained by the humid and wet climate in the northern DBF sites during summer. Located in the Midwest and Northeast, these sites have a relatively humid continental climate with considerable precipitation year-round, with precipitation in summer ranging from 2.73 to 3.79 mm/day and VPD from 0.73 to 1.09 kPa. As a result, LUE remains high in summer, and shows little interannual variability at each site.

In contrast to DBFs, ENF sites are distributed across most of the US other than the Midwest, with 22 sites in the south and 9 in the north. As expected, temperature exerted a stronger constraint on LUE in the colder climate in the north ($r = 0.82$) compared to the warmer climate in the south ($r = 0.78$) (Figure 4). Among them, 10 of the 22 southern sites are in the southwest, and all of them are at high elevations (2,015–3,050 m) with rather low temperature. In spring, the LUE increased with rising temperature at these cooler sites when it was below 10°C, reaching 0.3 g C/MJ in the southwest and 0.7 g C/MJ in the north (Figure 4). However, at the warmer and wetter ENFs in the southeast, the correlation between the LUE and temperature or SWA was insignificant in spring. In summer, it is clear that SWA$_{deep}$ drives LUE variations in both the north and south. Meanwhile, the rising temperature no longer positively affects LUE. Instead, elevated temperature hinders plant LUE at most sites. Interestingly, the spatial variation of summer LUE across most ENF sites differs substantially from the interannual variation in their relationship with temperature. Specifically, while the ENFs in the warm and humid Eastern US (with temperature above 20°C and SWA$_{deep}$ above 0.4) have higher LUE than in the cooler, drier Western US (with temperature below 20°C and SWA$_{deep}$ below 0.4), at a given site higher temperatures correspond with lower LUE. This seeming discrepancy between spatial and temporal variability may have resulted from the confounding effect of cross-site differences in LAI and water availability.

This study also compared six MF sites distributed across the United States, including Northeast, Midwest, Southern California, and Alabama locations. However, no clear pattern of LUE response to temperature and SWA was found, and the results were inconclusive due to the limited data available and the vast variability in climate and terrain conditions across the various sites.

The 10 northern GRA sites spread across the West and Midwest. During spring in the northern US, the variation in LUE is driven by both temperature and SWA$_{deep}$, and has a correlation coefficient of 0.79 with temperature and 0.87 with SWA$_{deep}$ (Figure 5). Multi-variate linear regression between LUE and the two predictors produced an R^2 of 0.84, indicating that ~84% of the LUE variance can be explained by the joint effects of temperature and SWA$_{deep}$. During summer, the variation in temperatures is small and has negligible impact on LUE, while

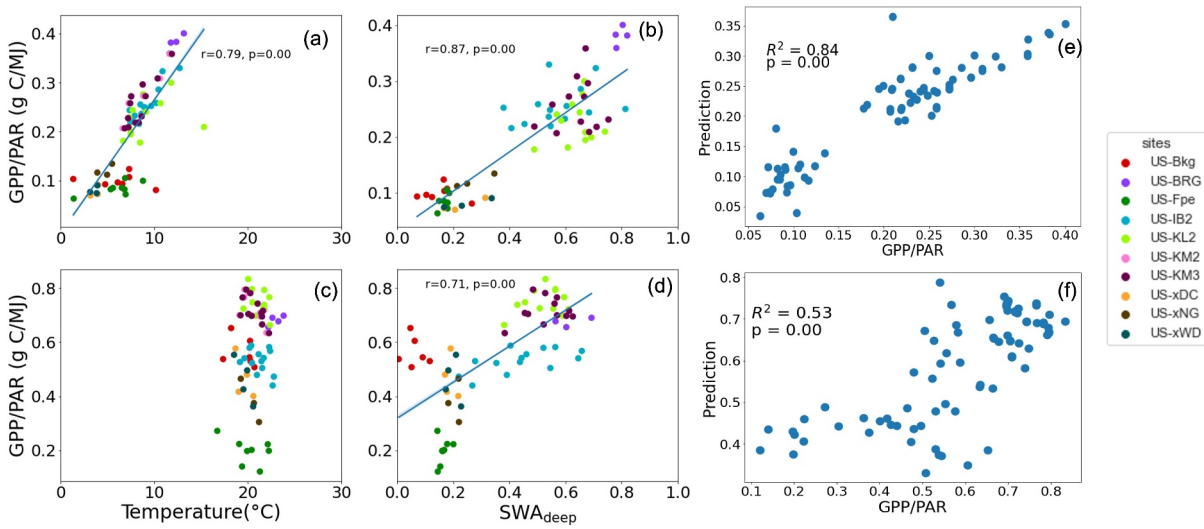

Figure 5. The relationship between seasonal mean LUE and seasonal mean temperature and SWA$_{deep}$ in GRAs during spring (a)–(b) and summer (c)–(d) in the Northern US, where different flux tower sites are distinguished by color; the relationship between the predicted value of the multivariate regression and the true value of LUE (e)–(f). The values in panels are for the Pearson correlation coefficient (r), its significance level (p), and the coefficient of determination (R^2).

SWA$_{deep}$ varied widely between sites and dominated the spatial variation in LUE, with higher productivity at wetter sites. An exception is observed at US-Bkg, where grassland maintains a high LUE at low SWA$_{deep}$. This might be due to the presence of C4 grass in US-Bkg. Vegetation at US-Bkg consists of a mixture of C3 and C4, and C4 plants have stronger heat and water stress adaptability, leading to high water use efficiency and production potential even under the influence of severe drought.

In the southwest, a hot and dry region, there is no consistent relationship between grass LUE and temperature during spring or summer (Figure 6). Located on diverse terrains including mountains, canyons, plateaus, and deserts, the southwestern sites exhibit significant variations in temperature and precipitation, which create distinct climatic niches. For example, at US-NR3, at a high elevation with below-freezing winter, temperature is the primary driver of LUE during the spring and summer. For the rest of the Southwest GRAs, temperature variations were small in spring, ranging from 13°C to 20°C, and did not have a major impact on LUE. However, SWA$_{deep}$ varied widely between sites, and this dominated the LUE spatial variations in spring. In arid regions, LUE in both spring and summer is typically lower than at wetter sites. In summer, LUE variations at relatively wet sites were driven by higher temperatures and reduced soil water availability. Despite the significant temperature differences among the southwestern GRAs sites (ranging from 10°C to 28°C), they exhibited similar LUEs. This may have to do with the differences in heat adaptability, as some are better adapted to hotter or cooler temperatures than others. For instance, at a site in California (US-SCg), the onset of heat stress occurs at 13°C, while at a site in Arizona (US-SRG), heat stress starts at 25°C.

In the southeast, a warm and humid region, the correlation between grass LUE variation and temperature or SWA$_{shallow}$ was weak or insignificant in spring (Figure 6). In summer, a negative effect of rising temperature on LUE was observed, with a correlation coefficient of −0.78; LUE was also constrained by SWA$_{shallow}$, with a correlation coefficient of 0.83. According to the multivariate regression, temperature and SWA$_{shallow}$ together explained 80% of the LUE variance, with generally higher LUE at wetter and cooler sites.

For ecosystems where both temperature and water availability are important drivers of LUE variation, the LUE relationship with either one of the variables cannot exclude the impact of the other. For a clear visualization of the separate effects of temperature and SWA on LUE, we analyzed the LUE variability across different combinations of temperature and SWA. Figure 7 shows the results for SWA$_{deep}$ as an example. In spring, the lowest LUE consistently occurred under rather extreme conditions: temperatures below zero for ENFs and below 4–8°C for other vegetation types, or soil water availability below 0.1 for grass. Above these thresholds, LUE increased with temperature for all three vegetation types and also increased with water availability for grass. The LUE variation at

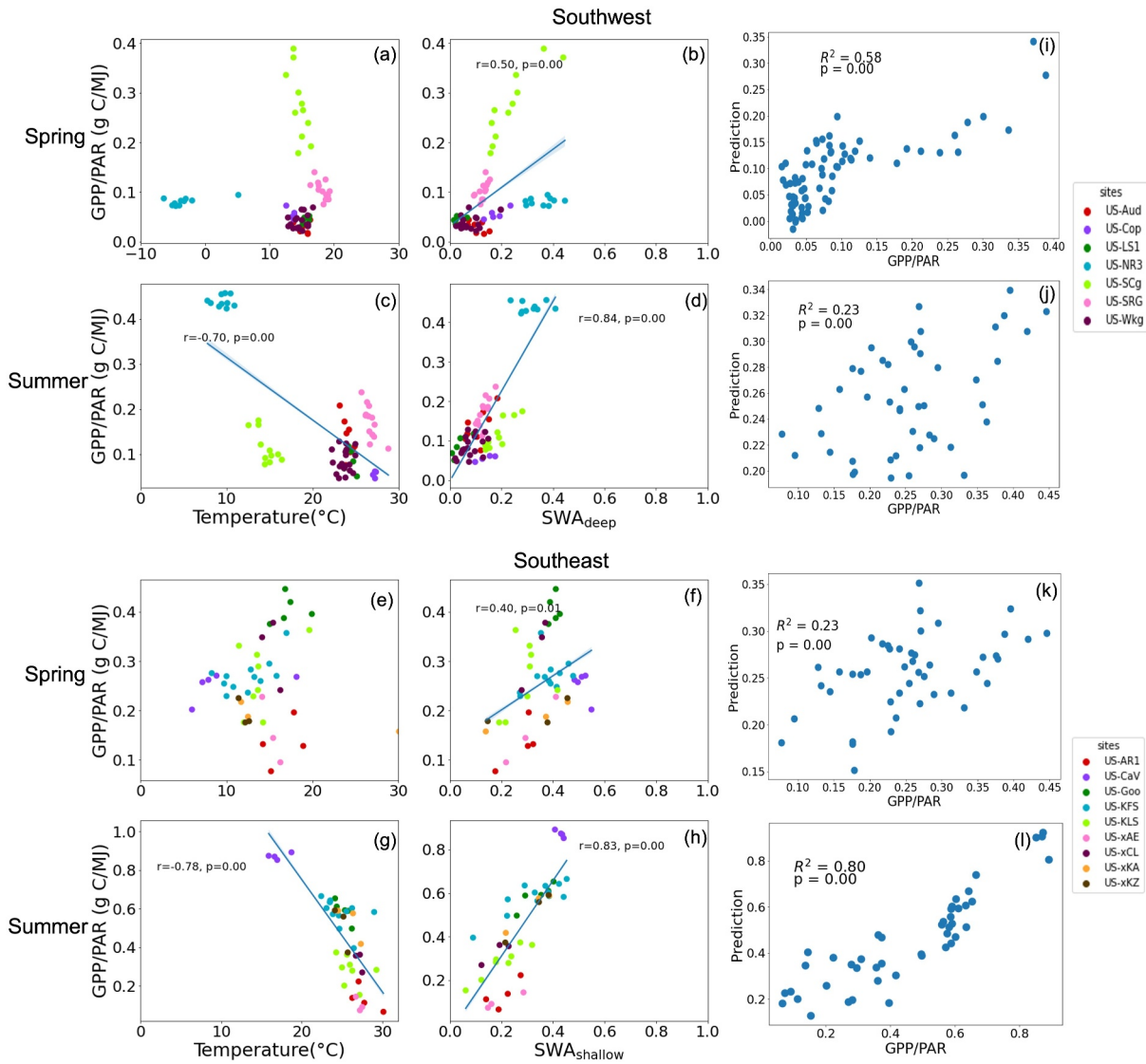

Figure 6. The relationship between seasonal mean LUE and seasonal mean temperature and SWA (at top 200 cm in the Southwestern US (a)–(d), at top 10 cm in the Southeastern US (e)–(h)) in GRAs during spring and summer, where different flux tower sites are distinguished by color; the relationship between the predicted value of the multivariate regression and the true value of LUE (i)–(l). The values in panels are for the Pearson correlation coefficient (r), its significance level (p), and the coefficient of determination (R^2).

GRA sites was clearly driven by both temperature and SWA_{deep}. At both the ENF and DBF sites, LUE showed little variation with SWA_{deep}, which is consistent with the results in Figures 3 and 4.

In summer, LUE variation at both the ENF sites and GRA sites was primarily driven by SWA_{deep}, and showed little temperature dependence. GRAs also encountered frequent compound heat-drought extremes when high temperatures coincided with low SWA_{deep}, resulting in very low LUE values; in contrast, such compound extremes are rare for ENF and DBF sites. Instead, DBF sites experienced apparent heat stress, with lower LUE values at high temperatures and no clear dependence on SWA. Additionally, the number of data points under extremely high temperatures with low SWA_{deep} is very small, which may cause uncertainty and potential biases.

3.3. The Role of Atmospheric Dryness

In addition to SWA_{deep}, atmospheric aridity is another drought factor influencing plant physiological processes. However, high VPD often coincides with low soil moisture and high temperature, and the three are tightly

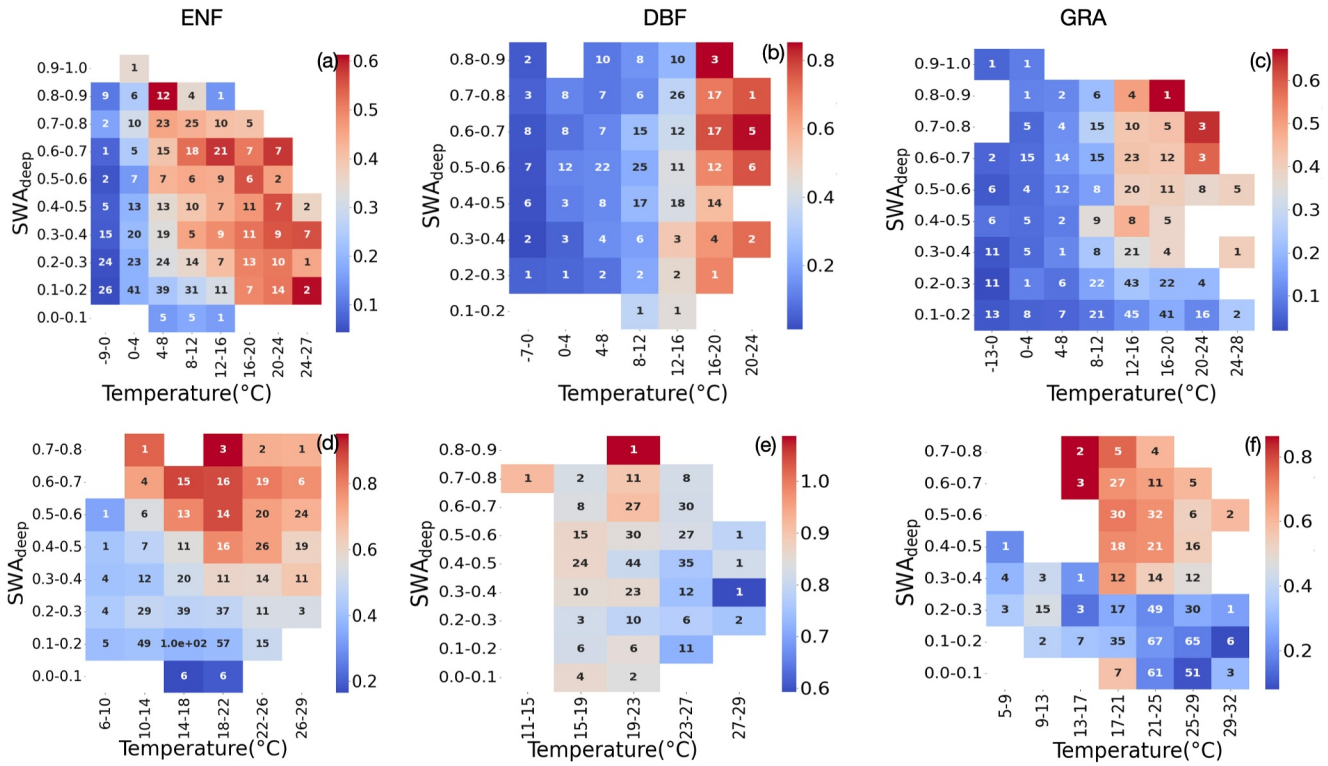

Figure 7. The variation in LUE (in gC/MJ) across different temperature and SWA_{deep} ranges in spring (a)–(c) and summer (d)–(f). The integer within each box represents the count of data points within each bivariate bin, and the color scale represents the GPP/PAR values averaged within each bin.

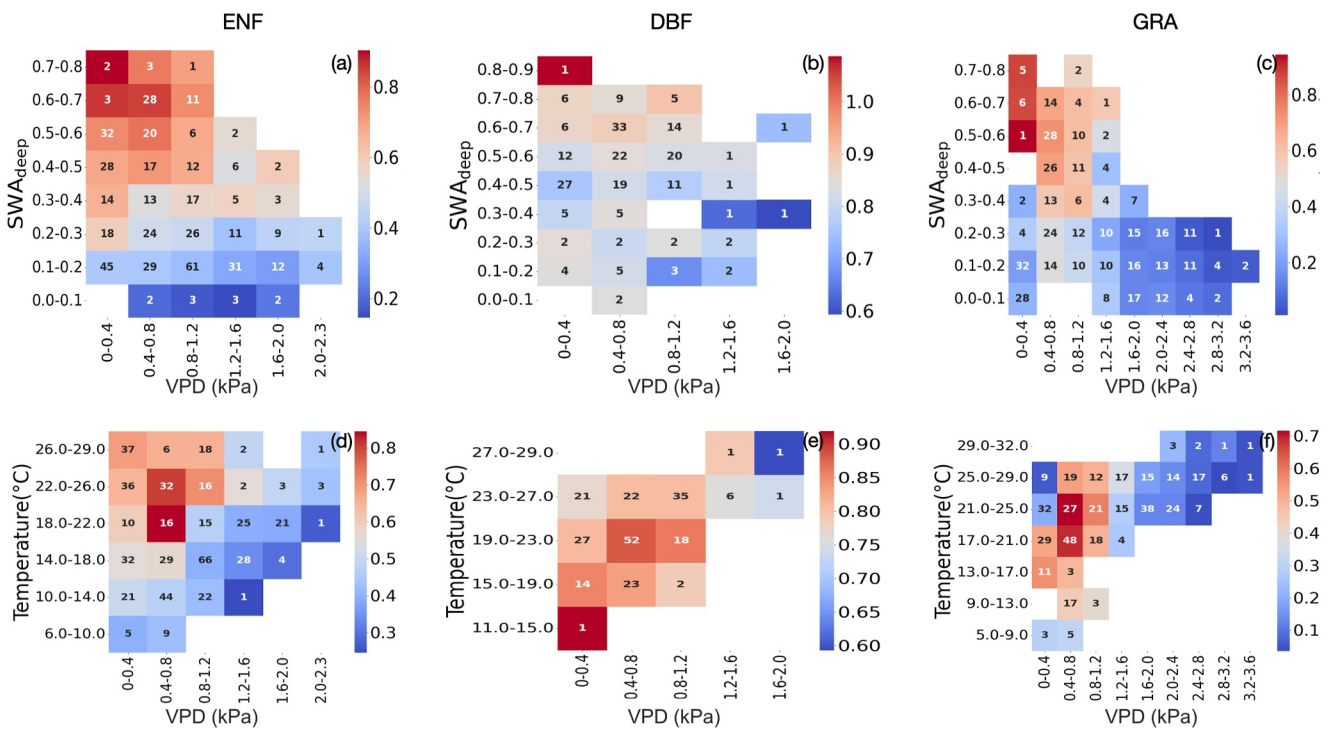

Figure 8. The variation of summer LUE (in gC/MJ) across different VPD and SWA_{deep} ranges (a)–(c) and across different VPD and temperature ranges (d)–(f). The integer within each box represents the count of data points within each bivariate bin, and the color scale represents the GPP/PAR values averaged within each bin.

coupled through evapotranspiration. It is not clear how SWA, temperature, and VPD may interact to influence plant photosynthesis (Zhou et al., 2019). Here we attempted to assess the role of VPD by separating its effects from those of SWA_{deep} or temperature (Figure 8), focusing on the summer season when the impact of water stress or aridity is the strongest. Not surprisingly, for all three vegetation types, the highest LUEs coincided with high SWA_{deep} and low VPD, while the lowest LUEs coincided with low SWA_{deep} and high VPD. The impact of SWA_{deep} appeared to dominate over the impact of VPD, especially at the ENF sites and for moderate aridity conditions at the GRA sites. However, under extreme drought conditions (low SWA_{deep}) at the GRA sites, atmospheric aridity was the dominant driver of LUE response, with a threshold of approximately 1.6 kPa; when VPD exceeded this threshold, LUE dropped significantly. The high VPD at the GRA sites also coincided with high temperature; however, as evident from Figure 8 (f), the impact of high VPD dominates over heat stress, causing extremely low LUE during compound heat-drought events. Specifically, under low VPD (<1.6 kPa) conditions, the impacts of soil water stress and heat stress were evident, with LUE increasing with SWA and temperature until the optimal temperature and then decreasing due to heat stress; under high VPD (>1.6 kPa) conditions, LUE showed little variation along the SWA gradient or temperature gradient (Figures 8c–8f). In contrast, except for the saturation conditions (VPD < 0.4 kPa), increasing VPD caused LUE to decrease regardless of the SWA and temperature conditions (Figures 8c–8f). At the forest sites (i.e., ENFs and DBFs), compound heat-drought conditions are rare so the results may not be robust due to the small sample size of LUE when VPD is high.

4. Conclusions

In this study, we examined the role of SWA, temperature, and atmospheric aridity in driving GPP variations of different vegetation types (ENF, DBF, and GRA) during the spring and summer in the United States, and used LUE as a standardized metric of GPP to enable comparison across different locations. Our analysis identified temperature as the dominant driver in spring, and SWA and VPD as the primary drivers in summer. During mild conditions of atmospheric aridity, the impact of drought on vegetation was dominated by soil water availability; under more severe aridity conditions at the GRA sites, VPD dominates the LUE response and is the primary cause for the loss of photosynthesis during extreme heat-drought compound events. All vegetation types are subjected to heat stress in the southern region. Temperature and soil water availability can explain a large fraction of the LUE variances in some ecosystems and some seasons or regions, but fail in others. More robust approaches such as machine learning may be necessary to better explore the predictive power of the different environmental factors.

In most years, ecosystems' transition from spring to summer resulted in a shift in the seasonal drivers of LUE variations from temperature dominance to SWA dominance. During spring, when the water supply is high, rising temperature positively affects LUE. However, during the summer season, the impact of rising temperature on LUE may vary in both the direction and the magnitude across different ecosystems, likely due to their thermal optimum differences. Ecosystems in the north reach or approach the optimal temperature with minimal LUE variations in summer, while ecosystems in the south may experience temperatures exceeding their thermal optimum and light saturation, consequently leading to a drop in LUE. As global warming continues to intensify, it is anticipated that the negative correlation between temperatures and LUE will become more pronounced in summer. Additionally, high temperatures in summer are often accompanied by high VPD, which may accelerate evapotranspiration and therefore soil moisture depletion thus limiting LUE; in addition, excessive VPD might induce stomatal closure thus severely limiting LUE. Therefore, the correspondence between low LUE and high temperature may not necessarily reflect the presence of heat stress. On the other hand, in the wet-to-dry transition region or seasons, increased VPD would initially reduce stomatal conductance to transpiration thus enhancing water use efficiency, slowing down the photosynthesis response to aridity (Xu et al., 2023a, 2023b; Zhang et al., 2019).

The variations observed in LUE response to temperature and SWA are site- and ecosystem-specific, show nonlinearity in many cases, and depend on background climate as well. Different regions and vegetation types possess distinct climatic niches, vegetation hydraulic properties, and heat tolerance, which influence the factors driving LUE variation. For example, at high altitudes, LUE is limited by spring snow cover and surface soil moisture. From the results in ENFs, DBFs and GRAs, temperature has a stronger constraint on LUE variations

in the cooler northern region than in the warmer southern region in spring. In summer, LUE in ENFs varies along the temperature gradient, with higher LUE at warmer sites. Our study shows that there is substantial spatial variability in the sensitivity of LUE to temperature across widely distributed ENFs in the United States. Further research is needed to understand how ENFs in different biota respond to climate change (Wagle et al., 2016a, 2016b). Additionally, the relevant depth of available soil water for plants varies across different regions. Apart from the northern grasslands, LUE in other ecosystems (including forests and southern grassland) is constrained by SWA_{deep}. This supports and supplements the recent finding of Xu et al. (2023a, 2023b) that using surface-layer soil moisture alone underestimates the soil moisture effects for deep-rooted plants.

5. Discussion

Further investigation is needed to understand the reasons behind the variations in LUE in certain ecosystems, such as southeastern ENFs, northern DBFs, and southeastern GRAs. One possible reason for the insignificant correlation between LUE and climate factors in these ecosystems may be their differential responses to major climate variables due to the substantial differences in forest age, land use history, topography, edaphic and climatic conditions, and species composition. For example, ENFs in the southeast are warmer than in the southwest. Within the same vegetation types, we observed a large spatial variability in SWA among southeastern ENF sites in spring, ranging from 0.1 to 0.8. Those distinct hydroclimatological conditions lead to large differences in response to climates in southeastern ENFs, and generalized vegetation types cannot capture the differences in sensitivity of different species to climate (Wagle et al., 2016a, 2016b). In northern DBFs, summer LUE is maintained at a high level with small variation, despite the clear variability of the climatic drivers examined in this study. It is unclear what may be responsible for this high degree of stability.

In addition, analyses based on the monthly and seasonal mean data smooth out the maximal GPP values, especially in DBFs and GRAs, which have high seasonal variability of LAI, leading to an underestimation of peak productivity and obscuring important ecological dynamics (see Figure S7 in Supporting Information S1). Focusing on the roles of climatic drivers in the spatiotemporal variability of GPP for different vegetation types, our study did not account for the impact of plant species, ages, or disturbances caused by pests, fire, or extreme storm events. Another limitation of this study is the data uncertainty. The FLUXCOM GPP data and NLDAS2 soil moisture data are both gridded products resulting from combining observations with models, and cannot account for the strong spatial heterogeneity expected of site-level data. Compared to GPP from the Ameriflux data set, FLUXCOM underestimated the peak productivity, especially in southern regions (see Figures S2 and S3 in Supporting Information S1). Soil moisture data at the flux tower sites are very limited, and vary in sensor type and measuring depth, hindering comparison across sites. Among the AmeriFlux sites, only the NEON sites offer consistent vertical profiles of soil moisture measurements, but NEON has been in operation for a short period and cannot provide adequate samples for interannual variation yet. Consistent measurements of soil moisture are critical for multi-site comparisons. Also important are high quality data for soil properties at the flux tower sites such as wilting point, porosity, and field capacity.

Due to the short operating time of most flux tower sites, our result did not reflect the effect of climate change. Warming is causing an increasing trend for heat stress and a decreasing trend of SWA over most of the globe. As climate change continues, photosynthesis in some terrestrial ecosystems is increasingly limited by soil water availability even in seasons and regions that historically experienced no water stress. Ecosystems with temperature-dominated variations in LUE may transition to being dominated by combined heat and drought conditions. Low soil moisture and high temperature will further increase atmospheric aridity, an already strong limiting factor for photosynthesis in grassland ecosystems. These changes may lead to tighter coupling between the terrestrial carbon and water cycles, even as GPP acclimates to warming, ultimately altering GPP variations among seasons and diminishing the capacity of the terrestrial ecosystem as a carbon sink.

Data Availability Statement

The FLUXCOM GPP data (Jung, 2020) is available via https://www.bgc-jena.mpg.de/geodb/. The system requires registration, and the download link is sent to the registered email address only. The Ameriflux FLUXNET Network Dataset is available via ameriflux.lbl.gov. The CERES Photosynthetic Active Radiation data (Doelling et al., 2016) is available via https://doi.org/10.5067/TERRA+AQUA/CERES/SYN1DEGMONTH_L3.004A.

The North American Land Data Assimilation System Soil Moisture dataset (NLDAS project, 2022) is available via https://doi.org/10.5067/NOXZSD0Z6JGD. The North American Land Data Assimilation System Mosaic Soil Hydraulic Properties Datasets (Mitchell et al., 2004) are available via https://ldas.gsfc.nasa.gov/nldas. The AVHRR LAI data (Vermote & NOAA CDR Program, 2019) is available via https://doi.org/10.7289/V53776Z4.

Acknowledgments

We acknowledge the following AmeriFlux sites for their data records: US-AR1, US-Aud, US-Bkg, US-Blk, US-Blo, US-BRG, US-CaV, US-Cop, US-CPK, US-CWt, US-CZ2, US-CZ3, US-CZ4, US-DK2, US-DK3, US-Fmf, US-Fpe, US-Fuf, US-GBT, US-GMF, US-Goo, US-Ha2, US-HBK, US-Ho1, US-IB2, US-KFS, US-KL2, US-KLS, US-KM2, US-KM3, US-LS1, US-Me2, US-Me6, US-MMS, US-Moz, US-MRf, US-MtB, US-NC1, US-NC3, US-NR1, US-NR3, US-Oho, US-ONA, US-Pfa, US-SCf, US-SCg, US-Slt, US-SP1, US-SP2, US-SP3, US-SRG, US-Syv, US-UMB, US-Var, US-Vcm, US-Vcp, US-Vcs, US-WBW, US-WCr, US-Wkg, US-xAB, US-xAE, US-xBL, US-xCL, US-xDC, US-xDL, US-xJE, US-xKA, US-xKZ, US-xLE, US-xML, US-xNG, US-xNW, US-xRM, US-xRN, US-xSB, US-xSC, US-xSE, US-xSP, US-xST, US-xTA, US-xTR, US-xUN, US-xWD. In addition, funding for AmeriFlux data resources was provided by the U.S. Department of Energy's Office of Science. Also, we acknowledge the FLUXCOM carbon flux data set from Martin Jung. This study was supported by funding from the National Science Foundation Research Traineeship Program Team-TERRA at the University of Connecticut (DGE-2022036), the NSF Signal in the Soil program (1935599), and NASA (S2SHYD-21-0044). The authors thank the anonymous reviewers for their thorough and constructive comments on an earlier version of the paper.

References

Bernacchi, C. J., Pimentel, C., & Long, S. P. (2003). *In vivo* temperature response functions of parameters required to model RuBP-limited photosynthesis. *Plant, Cell and Environment*, *26*(9), 1419–1430. https://doi.org/10.1046/j.0016-8025.2003.01050.x

Bernacchi, C. J., Singsaas, E. L., Pimentel, C., Portis, A. R., Jr., & Long, S. P. (2001). Improved temperature response functions for models of Rubisco-limited photosynthesis. *Plant, Cell and Environment*, *24*(2), 253–259. https://doi.org/10.1046/j.1365-3040.2001.00668.x

Bielczynski, L. W., Łącki, M. K., Hoefnagels, I., Gambin, A., & Croce, R. (2017). Leaf and plant age affects photosynthetic performance and photoprotective capacity. *Plant Physiology*, *175*(4), 1634–1648. https://doi.org/10.1104/pp.17.00904

Bodman, R. W., Rayner, P. J., & Karoly, D. J. (2013). Uncertainty in temperature projections reduced using carbon cycle and climate observations. *Nature Climate Change*, *3*(8), 725–729. https://doi.org/10.1038/nclimate1903

Chen, A., Huang, L., Liu, Q., & Piao, S. (2021). Optimal temperature of vegetation productivity and its linkage with climate and elevation on the Tibetan Plateau. *Global Change Biology*, *27*(9), 1942–1951. https://doi.org/10.1111/gcb.15542

Choury, Z., Wujeska-Klause, A., Bourne, A., Bown, N. P., Tjoelker, M. G., Medlyn, B. E., & Crous, K. Y. (2022). Tropical rainforest species have larger increases in temperature optima with warming than warm-temperate rainforest trees. *New Phytologist*, *234*(4), 1220–1236. https://doi.org/10.1111/nph.18077

Crous, K. Y., Uddling, J., & De Kauwe, M. G. (2022). Temperature responses of photosynthesis and respiration in evergreen trees from boreal to tropical latitudes. *New Phytologist*, *234*(2), 353–374. https://doi.org/10.1111/nph.17951

Doelling, D. R., Sun, M., Nguyen, L. T., Nordeen, M. L., Haney, C. O., Keyes, D. F., & Mlynczak, P. E. (2016). Advances in geostationary-derived longwave fluxes for the CERES synoptic (SYN1deg) product [Dataset]. *The Atmospheric Science Data Center*. https://doi.org/10.5067/Terra+Aqua/CERES/SYN1degMonth_L3.004A

Dusenge, M. E., Wittemann, M., Mujawamariya, M., Ntawuhiganayo, E. B., Zibera, E., Ntirugulirwa, B., et al. (2021). Limited thermal acclimation of photosynthesis in tropical montane tree species. *Global Change Biology*, *27*(19), 4860–4878. https://doi.org/10.1111/gcb.15790

Fang, J., Kato, T., Guo, Z., Yang, Y., Hu, H., Shen, H., et al. (2014). Evidence for environmentally enhanced forest growth. *Proceedings of the National Academy of Sciences of the United States of America*, *111*(26), 9527–9532. https://doi.org/10.1073/pnas.1402333111

Frouin, R., & Pinker, R. T. (1995). Estimating photosynthetically active radiation (PAR) at the Earth's surface from satellite observations. *Remote Sensing of Environment*, *51*(1), 98–107. https://doi.org/10.1016/0034-4257(94)00068-X

Gitelson, A. A., & Gamon, J. A. (2015). The need for a common basis for defining light-use efficiency: Implications for productivity estimation. *Remote Sensing of Environment*, *156*, 196–201. https://doi.org/10.1016/j.rse.2014.09.017

Gratani, L. (2014). Plant phenotypic plasticity in response to environmental factors. *Advances in Botany*, *2014*, 1–17. https://doi.org/10.1155/2014/208747

Green, J. K., Seneviratne, S. I., Berg, A. M., Findell, K. L., Hagemann, S., Lawrence, D. M., & Gentine, P. (2019). Large influence of soil moisture on long-term terrestrial carbon uptake. *Nature*, *565*(7740), 476–479. https://doi.org/10.1038/s41586-018-0848-x

Grossiord, C., Buckley, T. N., Cernusak, L. A., Novick, K. A., Poulter, B., Siegwolf, R. T. W., et al. (2020). Plant responses to rising vapor pressure deficit. *New Phytologist*, *226*(6), 1550–1566. https://doi.org/10.1111/nph.16485

Hayes, D. J., Vargas, R., Alin, S., Conant, R. T., Hutyra, L. R., Jacobson, A. R., et al. (2018). Chapter 2: The North American carbon budget. second state of the carbon cycle report. https://doi.org/10.7930/SOCCR2.2018.Ch2

He, B., Chen, C., Lin, S., Yuan, W., Chen, H. W., Chen, D., et al. (2022). Worldwide impacts of atmospheric vapor pressure deficit on the interannual variability of terrestrial carbon sinks. *National Science Review*, *9*(4), nwab150. https://doi.org/10.1093/nsr/nwab150

Higgins, S. I., Conradi, T., & Muhoko, E. (2023). Shifts in vegetation activity of terrestrial ecosystems attributable to climate trends. *Nature Geoscience*, *16*(2), 147–153. https://doi.org/10.1038/s41561-022-01114-x

Hu, L., Montzka, S. A., Kaushik, A., Andrews, A. E., Sweeney, C., Miller, J., et al. (2021). COS-derived GPP relationships with temperature and light help explain high-latitude atmospheric CO_2 seasonal cycle amplification. *Proceedings of the National Academy of Sciences of the United States of America*, *118*(33), e2103423118. https://doi.org/10.1073/pnas.2103423118

Hu, Y., Xiang, W., Schäfer, K. V. R., Lei, P., Deng, X., Forrester, D. I., et al. (2022). Photosynthetic and hydraulic traits influence forest resistance and resilience to drought stress across different biomes. *Science of the Total Environment*, *828*, 154517. https://doi.org/10.1016/j.scitotenv.2022.154517

Huang, M., Piao, S., Ciais, P., Peñuelas, J., Wang, X., Keenan, T. F., et al. (2019). Air temperature optima of vegetation productivity across global biomes. *Nature Ecology & Evolution*, *3*(5), 772–779. https://doi.org/10.1038/s41559-019-0838-x

Humphrey, V., Berg, A., Ciais, P., Gentine, P., Jung, M., Reichstein, M., et al. (2021). Soil moisture–atmosphere feedback dominates land carbon uptake variability. *Nature*, *592*(7852), 65–69. https://doi.org/10.1038/s41586-021-03325-5

Jung, M. (2020). FLUXCOM global land carbon fluxes [Dataset]. *Data Portal of the Max Planck Institute for Biogeochemistry*. https://doi.org/10.17871/FLUXCOM_CarbonFluxes_v1

Jung, M., Koirala, S., Weber, U., Ichii, K., Gans, F., Camps-Valls, G., et al. (2019). The FLUXCOM ensemble of global land-atmosphere energy fluxes. *Scientific Data*, *6*(1), 74. https://doi.org/10.1038/s41597-019-0076-8

Kirschbaum, M. U. F. (2004). Direct and indirect climate change effects on photosynthesis and transpiration. *Plant Biology*, *6*(3), 242–253. https://doi.org/10.1055/s-2004-820883

Kullberg, A. T., Slot, M., & Feeley, K. J. (2023). Thermal optimum of photosynthesis is controlled by stomatal conductance and does not acclimate across an urban thermal gradient in six subtropical tree species. *Plant, Cell and Environment*, *46*(3), 831–849. https://doi.org/10.1111/pce.14533

Liu, L., Gudmundsson, L., Hauser, M., Qin, D., Li, S., & Seneviratne, S. I. (2020). Soil moisture dominates dryness stress on ecosystem production globally. *Nature Communications*, *11*(1), 4892. https://doi.org/10.1038/s41467-020-18631-1

Liu, Y., Wu, C., Wang, X., & Zhang, Y. (2023). Contrasting responses of peak vegetation growth to asymmetric warming: Evidences from FLUXNET and satellite observations. *Global Change Biology*, *29*(8), 2363–2379. https://doi.org/10.1111/gcb.16592

Lloyd, J., & Farquhar, G. D. (2008). Effects of rising temperatures and CO_2 on the physiology of tropical forest trees. *Philosophical Transactions of the Royal Society B: Biological Sciences*, *363*(1498), 1811–1817. https://doi.org/10.1098/rstb.2007.0032

Lu, X., Croft, H., Chen, J. M., Luo, Y., & Ju, W. (2022). Estimating photosynthetic capacity from optimized Rubisco–chlorophyll relationships among vegetation types and under global change. *Environmental Research Letters*, *17*(1), 014028. https://doi.org/10.1088/1748-9326/ac444d

Mitchell, K. E., Lohmann, D., Houser, P. R., Wood, E. F., Schaake, J. C., Robock, A., et al. (2004). The multi-institution North American Land Data Assimilation System (NLDAS): Utilizing multiple GCIP products and partners in a continental distributed hydrological modeling system. *Journal of Geophysical Research*, *109*(D7), D07S90. https://doi.org/10.1029/2003JD003823

Mohammadi Alagoz, S., Zahra, N., Hajiaghaei Kamrani, M., Asgari Lajayer, B., Nobaharan, K., Astatkie, T., et al. (2022). Role of root hydraulics in plant drought tolerance. *Journal of Plant Growth Regulation*, *42*(10), 6228–6243. https://doi.org/10.1007/s00344-022-10807-x

Monteith, J. L. (1972). Solar radiation and productivity in tropical ecosystems. *Journal of Applied Ecology*, *9*(3), 747. https://doi.org/10.2307/2401901

Moore, C. E., Meacham-Hensold, K., Lemonnier, P., Slattery, R. A., Benjamin, C., Bernacchi, C. J., et al. (2021). The effect of increasing temperature on crop photosynthesis: From enzymes to ecosystems. *Journal of Experimental Botany*, *72*(8), 2822–2844. https://doi.org/10.1093/jxb/erab090

Niu, S., Luo, Y., Fei, S., Yuan, W., Schimel, D., Law, B. E., et al. (2012). Thermal optimality of net ecosystem exchange of carbon dioxide and underlying mechanisms. *New Phytologist*, *194*(3), 775–783. https://doi.org/10.1111/j.1469-8137.2012.04095.x

Niu, S., Luo, Y., Fei, S., Montagnani, L., Bohrer, G., Janssens, I. A., et al. (2011). Seasonal hysteresis of net ecosystem exchange in response to temperature change: Patterns and causes. *Global Change Biology*, *17*(10), 3102–3114. https://doi.org/10.1111/j.1365-2486.2011.02459.x

NLDAS project. (2022). NLDAS Noah land surface model L4 monthly 0.125 x 0.125 degree V2.0 [Dataset]. In D. M. Mocko (Ed.). https://doi.org/10.5067/WB224IA3PVOJ.*NASA/GSFC/HSL, Greenbelt, Maryland, USA, Goddard Earth Sciences Data and Information Services Center (GES DISC)*.

Pau, S., Detto, M., Kim, Y., & Still, C. J. (2018). Tropical forest temperature thresholds for gross primary productivity. *Ecosphere*, *9*(7), e02311. https://doi.org/10.1002/ecs2.2311

Peñuelas, J., Prieto, P., Beier, C., Cesaraccio, C., De Angelis, P., de Dato, G., et al. (2007). Response of plant species richness and primary productivity in shrublands along a north–south gradient in Europe to seven years of experimental warming and drought: Reductions in primary productivity in the heat and drought year of 2003. *Global Change Biology*, *13*(12), 2563–2581. https://doi.org/10.1111/j.1365-2486.2007.01464.x

Peñuelas, J., Rutishauser, T., & Filella, I. (2009). Phenology feedbacks on climate change. *Science*, *324*(5929), 887–888. https://doi.org/10.1126/science.1173004

Pinno, B. D., & Wilson, S. D. (2013). Fine root response to soil resource heterogeneity differs between grassland and forest. *Plant Ecology*, *214*(6), 821–829. https://doi.org/10.1007/s11258-013-0210-1

Rennenberg, H., Loreto, F., Polle, A., Brilli, F., Fares, S., Beniwal, R. S., & Gessler, A. (2006). Physiological responses of forest trees to heat and drought. *Plant Biology*, *8*(5), 556–571. https://doi.org/10.1055/s-2006-924084

Seleiman, M. F., Al-Suhaibani, N., Ali, N., Akmal, M., Alotaibi, M., Refay, Y., et al. (2021). Drought stress impacts on plants and different approaches to alleviate its adverse effects. *Plants*, *10*(2), 259. https://doi.org/10.3390/plants10020259

Stubbs, R. L., Soltis, D. E., & Cellinese, N. (2018). The future of cold-adapted plants in changing climates: *Micranthes* (Saxifragaceae) as a case study. *Ecology and Evolution*, *8*(14), 7164–7177. https://doi.org/10.1002/ece3.4242

Sulman, B. N., Roman, D. T., Yi, K., Wang, L., Phillips, R. P., & Novick, K. A. (2016). High atmospheric demand for water can limit forest carbon uptake and transpiration as severely as dry soil. *Geophysical Research Letters*, *43*(18), 9686–9695. https://doi.org/10.1002/2016GL069416

Sun, S., Du, W., Song, Z., Zhang, D., Wu, X., Chen, B., & Wu, Y. (2021). Response of gross primary productivity to drought time-scales across China. *Journal of Geophysical Research: Biogeosciences*, *126*(4), e2020JG005953. https://doi.org/10.1029/2020JG005953

Sun, X., & Wang, G. (2022). Causes for the negative scaling of extreme precipitation at high temperatures. *Journal of Climate*, *35*(18), 6119–6134. https://doi.org/10.1175/JCLI-D-22-0142.1

Turcotte, M. M., Corrin, M. S. C., & Johnson, M. T. J. (2012). Adaptive evolution in ecological communities. *PLoS Biology*, *10*(5), e1001332. https://doi.org/10.1371/journal.pbio.1001332

Turner, A. J., Köhler, P., Magney, T. S., Frankenberg, C., Fung, I., & Cohen, R. C. (2021). Extreme events driving year-to-year differences in gross primary productivity across the US. *Biogeosciences*, *18*(24), 6579–6588. https://doi.org/10.5194/bg-18-6579-2021

Vermote, E., & NOAA CDR Program. (2019). NOAA climate data record (CDR) of AVHRR surface reflectance, version 5 [Dataset]. *NOAA National Centers for Environmental Information*. https://doi.org/10.7289/V53776Z4

Vicente-Serrano, S. M., Gouveia, C., Camarero, J. J., Beguería, S., Trigo, R., López-Moreno, J. I., et al. (2013). Response of vegetation to drought time-scales across global land biomes. *Proceedings of the National Academy of Sciences of the United States of America*, *110*(1), 52–57. https://doi.org/10.1073/pnas.1207068110

Von Buttlar, J., Zscheischler, J., Rammig, A., Sippel, S., Reichstein, M., Knohl, A., et al. (2018). Impacts of droughts and extreme-temperature events on gross primary production and ecosystem respiration: A systematic assessment across ecosystems and climate zones. *Biogeosciences*, *15*(5), 1293–1318. https://doi.org/10.5194/bg-15-1293-2018

Wagle, P., Gowda, P. H., Xiao, X., & Anup, K. C. (2016b). Parameterizing ecosystem light use efficiency and water use efficiency to estimate maize gross primary production and evapotranspiration using MODIS EVI. *Agricultural and Forest Meteorology*, *222*, 87–97. https://doi.org/10.1016/j.agrformet.2016.03.009

Wagle, P., Xiao, X., Kolb, T. E., Law, B. E., Wharton, S., Monson, R. K., et al. (2016a). Differential responses of carbon and water vapor fluxes to climate among evergreen needleleaf forests in the USA. *Ecological Processes*, *5*(1), 8. https://doi.org/10.1186/s13717-016-0053-5

Wang, H., Yan, S., Ciais, P., Wigneron, J., Liu, L., Li, Y., et al. (2022). Exploring complex water stress–gross primary production relationships: Impact of climatic drivers, main effects, and interactive effects. *Global Change Biology*, *28*(13), 4110–4123. https://doi.org/10.1111/gcb.16201

Way, D. A., & Yamori, W. (2014). Thermal acclimation of photosynthesis: On the importance of adjusting our definitions and accounting for thermal acclimation of respiration. *Photosynthesis Research*, *119*(1–2), 89–100. https://doi.org/10.1007/s11120-013-9873-7

Wolf, S., Eugster, W., Ammann, C., Häni, M., Zielis, S., Hiller, R., et al. (2013). Contrasting response of grassland versus forest carbon and water fluxes to spring drought in Switzerland. *Environmental Research Letters*, *8*(3), 035007. https://doi.org/10.1088/1748-9326/8/3/035007

Wolf, S., Keenan, T. F., Fisher, J. B., Baldocchi, D. D., Desai, A. R., Richardson, A. D., et al. (2016). Warm spring reduced carbon cycle impact of the 2012 US summer drought. *Proceedings of the National Academy of Sciences of the United States of America*, *113*(21), 5880–5885. https://doi.org/10.1073/pnas.1519620113

Xia, Y., Mitchell, K., Ek, M., Sheffield, J., Cosgrove, B., Wood, E., et al. (2012). Continental-scale water and energy flux analysis and validation for the North American Land Data Assimilation System project phase 2 (NLDAS-2): 1. Intercomparison and application of model products. *Journal of Geophysical Research*, *117*(D3), D03109. https://doi.org/10.1029/2011JD016048

Xu, S., Gentine, P., Li, L., Wang, L., Yu, Z., Dong, N., et al. (2023a). Response of ecosystem productivity to high vapor pressure deficit and low soil moisture: Lessons learned from the global eddy-covariance observations. *Earth's Future*, *11*(8), e2022EF003252. https://doi.org/10.1029/2022EF003252

Xu, Z., Tian, Y., Liu, Z., & Xia, X. (2023b). Comprehensive effects of atmosphere and soil drying on stomatal behavior of different plant types. *Water*, *15*(9), 1675. https://doi.org/10.3390/w15091675

Yamasaki, T., Yamakawa, T., Yamane, Y., Koike, H., Satoh, K., & Katoh, S. (2002). Temperature acclimation of photosynthesis and related changes in photosystem II electron transport in winter wheat. *Plant Physiology*, *128*(3), 1087–1097. https://doi.org/10.1104/pp.010919

Zhang, Q., Ficklin, D. L., Manzoni, S., Wang, L., Way, D., Phillips, R. P., & Novick, K. A. (2019). Response of ecosystem intrinsic water use efficiency and gross primary productivity to rising vapor pressure deficit. *Environmental Research Letters*, *14*(7), 074023. https://doi.org/10.1088/1748-9326/ab2603

Zhang, Z., Zhang, R., Cescatti, A., Wohlfahrt, G., Buchmann, N., Zhu, J., et al. (2017). Effect of climate warming on the annual terrestrial net ecosystem CO_2 exchange globally in the boreal and temperate regions. *Scientific Reports*, *7*(1), 3108. https://doi.org/10.1038/s41598-017-03386-5

Zhou, S., Zhang, Y., Ciais, P., Xiao, X., Luo, Y., Caylor, K. K., et al. (2017). Dominant role of plant physiology in trend and variability of gross primary productivity in North America. *Scientific Reports*, *7*(1), 41366. https://doi.org/10.1038/srep41366

Zhou, S., Zhang, Y., Park Williams, A., & Gentine, P. (2019). Projected increases in intensity, frequency, and terrestrial carbon costs of compound drought and aridity events. *Science Advances*, *5*(1), eaau5740. https://doi.org/10.1126/sciadv.aau5740